Analytical Methods

Accepted Manuscript

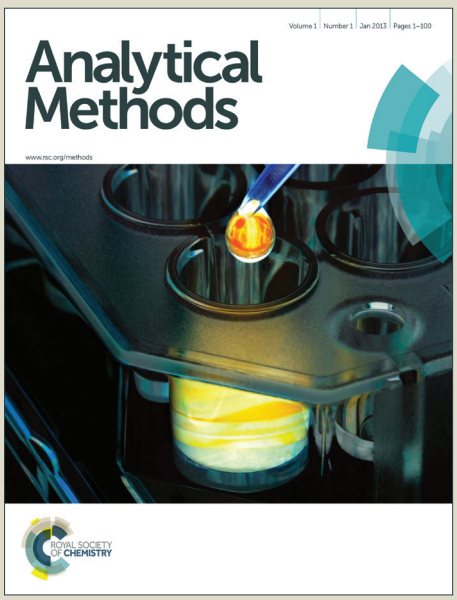

ROYAL SOCIETY OF CHEMISTRY

www.rsc.org/methods

Graphical Abstract

Fluorescence quenching studies of CTAB stabilized perylene nanoparticles for determination of Cr(VI) from environmental samples : Spectroscopic Approach

Dattatray K. Dalavi, D. P. Bhopate, A. S. Bagawan, A. H. Gore, N. K. Desai, A. A. Kamble, P. G. Mahajan, G. B. Kolekar, Shivajirao R. Patil*

Fluorescence Spectroscopy Laboratory, Department of Chemistry, Shivaji University, Kolhapur-416004 (India)

Abstract:

CTAB-PNPs are bound to the dichromate ion by electrostatic interaction to form non-fluorescent stable micellar complex which is responsible for the 'FL quenching' of CTAB-PNPs. We have demonstrated a different strategy to improve the fluorescence detection limit by the method based on 'FL quenching' of CTAB-PNPs.

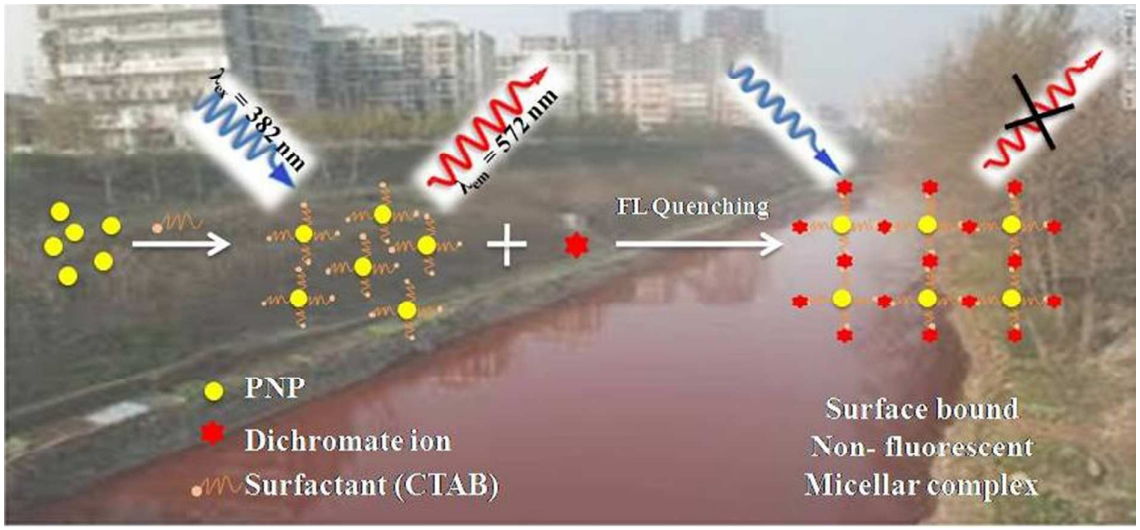

Fluorescence quenching studies of CTAB stabilized perylene nanoparticles for determination of Cr(VI) from environmental samples : Spectroscopic Approach

Dattatray K. Dalavi, D. P. Bhopate, A. S. Bagawan, A. H. Gore, N. K. Desai, A. A. Kamble, P. G. Mahajan, G. B. Kolekar, Shivajirao R. Patil*

Fluorescence Spectroscopy Laboratory, Department of Chemistry, Shivaji University, Kolhapur-416004 (India)

Abstract

Cetyl trimethyl ammonium bromide (CTAB) stabilized perylene nanoparticles (PNPs) were prepared by modified reprecipitation method in aqueous solution under ultrasonic treatment. A spectrofluorimetric method for the quantitative determination of hexavalent chromium [Cr(VI)] based on the fluorescence (FL) quenching of CTAB stabilized PNPs (CTAB-PNPs) by Cr(VI) as dichromate species in aqueous solution was proposed. Under the most favourable conditions, FL intensity of PNPs monitored at excitation wavelength λ_{ex} = 382 nm was quenched by successive addition of concentration of dichromate ions. The FL quenching results found to fit into Stern-Volmer (S-V) relation in the range of 0.5–50 μg mL^{-1} with a correlation coefficient of 0.9997. The limit of detection (LOD) was 0.008 μg mL^{-1}. The method based on FL quenching was successfully applied for quantitative analysis of Cr(VI) in water samples collected from different environment.

Keywords: Reprecipitation, cetyl trimethyl ammonium bromide stabilized perylene nanoparticles (CTAB-PNPs), FL quenching, dichromate ion, hexavalent chromium [Cr(VI)].

Corresponding author Tel.: +91-0231-2609061; fax: +91-0231-2692333.

***E-mail:** srp_fsl@rediffmail.com

1. Introduction

In natural media, chromium is usually found in trivalent and hexavalent oxidation states in soil, ground water and seawater.[1] Cr(III) is an essential element in mammals for maintaining efficient glucose, lipid, and protein metabolism.[2] On the other hand, Cr(VI) is toxic ion species which is a wide spread industrial pollutant. It comes into aquatic environments mostly through effluents from the electroplating, metal finishing industries, leather tanning, cooling tower blowdown, plating, inorganic chemical plants, textile manufacturing, anodizing baths, rinse waters, etc.[1-4] It can directly enter the drinking water supply scheme from the corrosion inhibitors used in the water pipes. Consequently, even if low concentration of Cr(VI) posses serious health risks, including damaging exposed skin, irritating mucous membranes, producing pulmonary sensitivity, creating dental erosion, inducing renal damage, targeting the respiratory track and skin.[5, 6] The guidelines prescribed by the World Health Organization (WHO) for Cr(VI) in drinking water is 16 mg/L.[7] The US Environmental Protection Agency recommends that the concentration of Cr(VI) in drinking water should be less than 0.1µg/mL.[8] Owing to highly toxicity and carcinogenicity for humans,[9] it is essential to undertake a precise and sensitive detection of Cr(VI) at trace level in the field of environmental science and industry. Several detection methods are available for the quantification of the total chromium or chromium species, including solvent extraction,[10] solid-phase extraction (SPE),[11] surface plasmon-enhanced resonance light scattering (SP-RLS),[12] flow injection solid phase extraction electrothermal atomic absorption spectrometry,[13] ion exchange,[14] flame atomic absorption spectrometry (FAAS),[15] electrothermal atomic absorption spectrometry (ETAAS),[16-19] inductively coupled plasma-atomic emission spectrometry (ICP-AES),[20,21] high performance liquid chromatography with inductively coupled plasma–mass spectrometry (HPLC-ICP-MS),[22] voltammetry,[23,24] label free colorimetric sensor,[10] luminescence,[25] chromatography and chemiluminescence,[26] and

fluorescence quenching.[5] Although, some of these techniques have high selectivity and sensitivity, they tend to be complicated, requires long analysis time and expensive to apply and some methods would lost the sensitivity when measuring low concentration of Cr(VI) in the presence of high concentration of Cr(III). Therefore, we have demonstrated a different strategy to improve the fluorescence detection limit of Cr(VI) by the method based on FL quenching of CTAB-PNPs.

Fluorescent organic nanoparticles (FONs) have attracted a great deal of research interests in recent years due to their peculiar size-dependent optical and electronic properties.[27-31] FONs have high potential applications because they allow much more variability and flexibility in material synthesis and nanoparticle preparation.[32] The various kinds of methods used for preparation of FONs such as emulsification evaporation, emulsification diffusion[31] and laser ablation.[33,34] Reprecipitation becomes a popular method for the preparation of organic nanoparticles because of its easy and versatile operation.[33] The process of reprecipitation method is carried out by rapidly injecting microamounts of the solution of organic compound in a good solvent into a poor solvent. The good solvent disperses and the sudden change of environment for organic molecules induce precipitation in the form of nano or microcrystal dispersion.[35]

In this paper, we report the preparation of PNPs in presence cationic surfactant CTAB. The method based on FL quenching of CTAB-PNPs by Cr(VI) is simple, less expensive, highly sensitive and reliable for quantification of the Cr(VI) in water samples collected from different environment, even in presence of high concentration of Cr(III).

2. Experimental

2.1. Reagents

Perylene was purchased from Sigma Aldrich. Cetyl trimethyl ammonium bromide (CTAB) procured from Spectrochem Pvt. Ltd. Mumbai. Potassium dichromate ($K_2Cr_2O_7$) was purchased from s d fine-chem Ltd. (Mumbai, India). The stock solution of dichromate ions was prepared by dissolving potassium dichromate ($K_2Cr_2O_7$) in water. All chemicals used were of analytical reagent grade and used as received without further purification. Doubly distilled water was used for preparing all solutions throughout the experiments.

2.2. Instrumentation

The absorption spectrum was acquired at room temperature on UV-3600 Shimadzu UV−VIS−NIR spectrophotometer with the use of 1.0 cm quartz cell. FL measurement of solutions was made with PC based spectrofluorophotometer (JASCO Model FP-8300, Japan). The excitation wavelength 382 nm was obtained from the excitation spectrum and the emission spectrum was monitored at this excitation wavelength. Both excitation and emission slits were fixed at 10 nm. The particle size distribution and zeta potential of PNPs in aqueous suspension was measured by dynamic light scattering (DLS) with a Zeta Sizer Nano ZS (Malvern Instruments Ltd., U. K.). A scanning electron microscope, SEM (JEON-6360 Japan) was used to examine the morphology and size of the nanoparticles. The pH of solutions was measured with digital pH meter model LI-120 (ELICO Hyderabad, India) with a combined glass electrode.

2.3 Preparation of CTAB-PNPs

CTAB-PNPs were prepared by the modified reprecipitation method.[28,30,35] 0.1 ml of a perylene solution in acetone (1 mM) was injected by a microsyringe into 100 ml CTAB aqueous solution (0.5 mM) with vigorously stirring at ambient temperature to assemble a pale-yellow colloid. Then the content was sonicated for 25 min at 301 K so as to obtain

dispersion of nanoparticles into water. Cationic surfactant CTAB acts as a stabilizer which helps to control nucleation growth of nanoparticles and avoid further aggregation of the nanoparticles into bigger molecules. Hence, stable colloidal dispersions of PNPs were formed in water.

3. Results and discussion

3.1. Morphology and particle size of PNPs

The particle size distribution of nanoparticles in aqueous suspension was examined by Dynamic Light Scattering (DLS). Fig. 1 (a) presents the particle size distribution of PNPs in aqueous suspension in the absence of surfactant. The particle size data shows the range of the particle size from 91.28 nm to 141.8 nm distribution of mean number % of particles from 18.1% to 6.9%. The maximum number mean % is 43.1 and the average particle size is 118 nm. Fig. 1 (b) presents the particle size distribution of PNPs in the absence of surfactant. The particle size data shows the range of the particle size from 17.17 nm to 28.21 nm distribution of mean number % of particles from 17.3% to 7.7%. The maximum number mean % is 42.3 and the average particle size is 22.18 nm.

Zeta (ζ) potential measurement was performed for PNPs in order to characterize the surface charge on the nanoparticles and stability of nanoparticle. Fig. 2 shows the zeta potential of the CTAB-PNPs as 31.7 mV and that of the PNPs without surfactants is -2.6 mV. The significance of zeta potential is that its value can be related to the stability of colloidal dispersions. The high zeta potential confers stability due to the tendency of solution or dispersion to resist aggregation. When the potential is low, attraction exceeds repulsion and the dispersion will break. Consequently, colloids with low zeta potentials tend to coagulate or flocculate while colloids with high zeta potential (negative or positive) are electrically stabilized.[36,37] In the present study, the high zeta potential of such dispersion confirm that the

nanoparticles are well stabilized by surfactant and no more aggregation takes place. The CTAB capped colloid of perylene nanoparticle has high level stability and narrow particle size distribution as compared to nanoparticle suspension formed without CTAB.

Fig. 3b presents the scanning electron microscope (SEM) photomicrograph of an air dried layer of PNPs in the presence of CTAB surfactant. The figure clearly shows that the aggregated particles are monodispersed and spherical in shape due to controlled growth of nanoparticles in the presence of CTAB surfactant and the average particle size estimated from the SEM image is 34 nm however uncontrolled growth of nanostructures is observed in the absence of CTAB surfactant presented in Fig. 3a and the average particle size estimated is 128 nm. The average particle size estimated from the SEM images is relatively greater than the size obtained from DLS record. This is due to agglomeration of the nanoparticles during drying of the suspension on the glass substrate in an attempt to obtain thin films.

3.2 Absorption Spectroscopy of CTAB-PNPs

The prepared CTAB-PNPs were characterized by the UV−visible absorption spectra. Fig. 4 shows UV-vis absorption spectra of PNPs in aqueous dispersion and homogeneous solution of perylene in acetone. The observation of the spectra in figure reveals that the absorption maximum appeared at 470 nm for PNPs is red-shifted from the structured spectrum of homogeneous solution of perylene in acetone with maximum at 434 nm. The absorption maximum of PNPs undergoes a slightly bathochromic shift to the lower energy side as compared that of monomeric absorption. In general, because of light scattering effects of a relatively large colloidal solution with a strong absorption, the absorption appears to shift from its molecules in solution to a longer wavelength.[31] The bathochromic shift indicates that the molecules undergo aggregation in PNPs. Moreover, the absorption spectrum of PNPs

showed no apparent change for more than a month, which means that the nanoparticles dispersed stably in aqueous solution of surfactant.

3.3 FL Properties of CTAB-PNPs

Fig. 5 presents structured emission spectrum of dilute solution of isolated perylene molecules in acetone monitored at excitation wavelength, λ_{ex} = 410 nm and that of PNPs in aqueous suspension monitored at excitation wavelength, λ_{ex} = 382 nm obtained from its FL excitation spectrum shown in the Fig. 6a(A). The structured FL spectrum of perylene solution shows two prominent bands at 445 nm (λ_1) and 475 nm (λ_2). In addition to these bands, one weak band at 510 nm and a shoulder at 545 nm are seen in the spectrum due to less probable transition. However, FL spectrum of PNPs revels strong aggregation induced enhanced emission broad band peaking at 572 nm and weak bands of perylene monomer at 445 nm and 475 nm. These spectral properties clearly indicate that the monomer emission of perylene at λ_1 and λ_2 are quenched and emission of nanostructure at 572 nm (λ_3) becomes prominent. This red shifted emission is due to aggregated molecules of perylene nanostructure is explained on the basis of the fact that the electronic of aggregated molecules occurring from zeroth vibrational level of first electronic excited to zeroth vibrational level of ground state (0-0, 0-1) is shifted to the higher vibronic state of ground electronic state (0-2, 0-3).[38]

The Stoke's shift estimated from Fig. 6a and Fig. 6b as a difference between excitation and FL energy for PNPs suspension is $\Delta\bar{\upsilon}$ = 8833.27 cm^{-1} and for dilute solution of perylene in acetone is $\Delta\bar{\upsilon}$ = 355.9 cm^{-1} respectively. The large Stoke's shift is considered as aggregation of molecules by π-stacking effects to form nanocluster. The enhanced emission is become of restricted rotation of molecules which prevents dissipation of energy nonradiatively and hence radiative route is favoured in aggregated molecules and FL intensity on aggregation is enhanced (AIEE).

3.4 Effect of pH value

It is known that Cr(VI) exists in two anionic forms such as $Cr_2O_7^{2-}$ and CrO_4^{2-} in the water matrix. CrO_4^{2-} is stable in alkaline or neutral pH, while $Cr_2O_7^{2-}$ in acidic conditions. Similarly it is well known that chromate ion can convert into dichromate ion under acidic conditions and vice versa as expressed in following equation.[1]

$$2CrO_4^{2-} + 2H^+ \leftrightarrow Cr_2O_7^{2-} + H_2O \quad \text{.....,(1)}$$

Due to this the FL quenching experiments were performed under acidic condition using dichromate ion instead of chromate ion. The effect of pH value of the solution on the FL intensity of CTAB-PNPs in the presence of dichromate ions (1.0 μg mL^{-1}) was studied between pH 1.0 to 12 with different buffers and it was found that the most sensitive pH lies in the acidic range of 3.5−5.5 with NaAc-HAc buffer as shown in Fig. 7. Therefore, for every measurement in the present work NaAc-HAc solution having pH = 4.5 was chosen to run the assay. Moreover, the reaction is very fast and completed within a few seconds at room temperature. A constant maximum absorbance and emission intensity were obtained just after the addition of Cr(VI) and remained unaltered for 24 h.

3.5 Selective FL quenching of PNPs by Cr(VI)

To develop analytical method based on FL quenching for estimation of Cr(VI), we have prepared positively charged PNPs using the modified reprecipitation method in the presence of soft templates of the CTAB surfactant. Several numbers of the species are present in waste-water as well as industrial effluents and they may have the potential to quench FL emission of the probe. To explore the selectivity of the proposed method using PNPs as a probe for Cr(VI) in aqueous solution, the interference of some common ions on FL intensity of the probe in presence of each ion was studied separately under the chosen conditions. Fig.

8 shows that the changes in FL intensity of the probe were measured in the presence of various co-existing ions like Cr(III), Al(III), Ba(II), Fe(III), Zn(II), Na(I), Hg(II), Ni(II), Cu(II), Co(II), K(I), NO_3^-, Cl^-, SO_4^{2-}, CO_3^{2-}, BrO_3^-, IO_3^-, ClO_3^- etc. The Most of these ions have negligible interference in the present study which reveals that the method is more sensitive and precise for the analysis of Cr(VI) in different environmental water samples without separation of Cr(III), liquid mercury etc.

3.6 Calibration curve, limit of detection (LOD) and precision

The development of new analytical technique of high sensitivity and selectivity is always a challenge in analytical chemistry. Under the optimal experimental conditions as mentioned above, the FL emission spectra using CTAB-PNPs as a probe with different amounts of Cr(VI) in dichromate species were recorded in Fig. 9. The FL intensity of the probe was significantly quenched regularly without any spectral shift by gradual addition of dichromate ion solution in the range of concentration 0 - 50 μg mL^{-1}.

The quenching results fit into the conventional linear Stern-Volmer relationship.

$$F_0 / F = K_{SV}[Q] + 1 \quad \text{.....(2)}$$

Where F_0 is the FL intensity of the fluorophore in the absence of quencher and F is the FL intensity of the fluorophore when the quencher is present at concentration [Q]. K_{sv} is the Stern-Volmer quenching constant. The plot of changes in FL intensity (F_0/F) versus concentration of dichromate ions as shown in Fig. 10. The obtained experimental data for Cr(VI) determination fitted well to the following empirical equation.

$$F_0 / F = 0.151x + 1 \quad \text{.....(3)}$$

The linear relationship in the range of 0.5–50 μg mL^{-1} has a correlation coefficient of $R^2 = 0.9997$ (n = 4). The limit of detection based on the definition by equation,

$$LOD = 3.3\sigma / k \quad \text{.....(4)}$$

where σ is the standard deviation of the y- intercepts of the regression lines and k is the slope of calibration graph. Here the LOD was 0.008 μg mL^{-1}. This presented FL quenching method is more sensitivity and selectivity because of strong aggregation induced enhanced emission of PNPs and surface modification done by CTAB capping. The method has advantages of lower detection limit (LOD) and wide linear range of concentration for Cr(VI) without separation of Cr(III) over the existing methods and is illustrated in Table 1.

3.7 FL quenching mechanism

To explore the plausible mechanism of FL quenching, the FL spectra of CTAB-PNPs were investigated in the absence and presence of dichromate species. Careful observation of Fig. 9 reveals λ_3 attributed to the emission arising from nanoparticle is quenched significantly and regularly with addition of dichromate ion solution in the range of concentration 0.5- 50.0 μg mL^{-1} while that of λ_1 and λ_2 seen to be weakly quenched and irregular. As per the binding mode, it was demonstrated that CTAB modifies the surface of the monodispersed nanoparticles and bound to the dichromate ion by electrostatic interaction to form non-fluorescent stable micelle complex in ground state which is responsible for the quenching of CTAB-PNPs (eqn (5)).

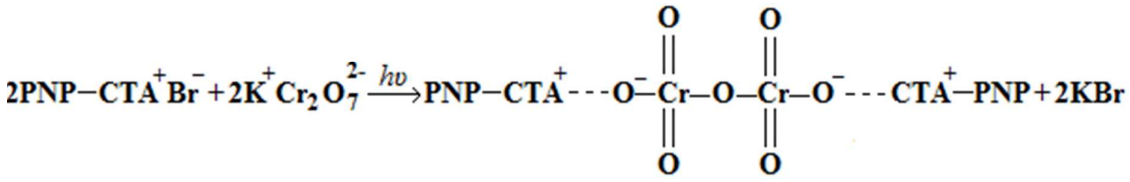

…… (5)

The possible FL quenching mechanism of CTAB-PNPs by solution of dichromate species and formation of non-fluorescent micellar complex is summarized in the Scheme 1.

3.8 Applications of proposed method for determination of Cr(VI) in environmental samples

Under the most favourable conditions mentioned above, the present method was fruitfully applied to determine Cr(VI) from synthetic and different environmental water samples by a standard addition method. The results obtained for the synthetic samples are shown in Table 2. The method has good recovery in the linear range which demonstrated the proposed method is free from interference of Cr(III) and the precision is ascertained by calculating the relative standard deviation (RSD) of four replicate determinations. Table 3 shows, the results obtained for the waste-water samples 1 and 2, those were collected from industrial effluents of textile and dyes industries (Ichalkaranji, West Maharashtra, India). Recovery of the method was verified by analyzing the water samples by the AAS standard method recommended for the determination of Cr(VI) in water. Recovery values obtained are in the range 98.95–100.15%, which demonstrated that the method based on the FL quenching of CTAB-PNPs can effectively recognize Cr(VI) over other co-existing ions in aqueous media.

4. Conclusions

CTAB-PNPs prepared by reprecipitation method was applied successfully as a fluorescent probe for the determination of Cr(VI) from water samples using FL quenching method. Furthermore, it is mostly effective at measuring low concentration of Cr(VI) in the presence of high concentration of Cr(III) as well as mercury with a detection limit of 0.008 $\mu g\ mL^{-1}$. The calibration curve is linear over the concentration range 0.5–50 $\mu g\ mL^{-1}$ with a correlation coefficient of 0.9997. The developed method is simple, rapid, reproducible, selective and free from interference of excipients. The content of Cr(VI) in synthetic and environmental samples determined by the present method agreed with the reference method with satisfactory recovery.

Acknowledgements

We gratefully acknowledge Department of Science and Technology, Delhi and University Grants Commission, Delhi for providing funds to Department of Chemistry under FIST and SAP-DRS Phase-II program, respectively.

References

1 A. F. Zheng, J. L. Chen, G. Wu, G. Wu, Y. G. Zhang, H. P. Wei, *Spectrochimica Acta Part A,* 2009, **74**, 265-270.

2 Ronald Eisler, *Biological Report,* 1986, **85**.

3 A. K. Singh, V. K. Gupta, Barkha Gupta, *Analytica Chimica Acta*, 2007, **585**, 171-178.

4 D. Mohan, C. U. Pittman Jr., *Journal of Hazardous materials*, 2006, **137**, 762-811.

5 T. M. A. Razek, S. Spear, S. S. M. Hassan, M. A. Arnold, *Talanta*, 1999, **48**, 269–275.

6 http://www.engr.uconn.edu/~baholmen/docs/ENVE290W/National%20Chromium%20Files%20From%20Luke/Cr(VI)%20Handbook/L1608_C08.pdf

7 WHO, *Guidelines for Drinking Water Quality*, Recommendations, World Health Organization, Geneva, 3rd edn, 2004, **1**.

8 Fei-Ming Li, Jia-Ming Liu, Xin-Xing Wang, Li-Ping Lin, Wen-Lian Cai, Xuan Lin, Yi-Na Zeng, Zhi-Ming Li, Shao-Qin Lin, *Sensors and Actuators B*, 2011, **155**, 817-822.

9 A. Zhitkovich, *Chem. Res. Toxicol.*, 2011, **24**, 1617.

10 M. A. Elbagermi, A. I, Alajtal, H. G.M. Edwards, *APCBEE Procedia*, 2013, **5**, 378-382.

11 A. Bartyzel, E. M. Cukrowska, *Analytica Chimica Acta*, 2011, **707**, 204-209.

12 Z. Han, L. Qi, G. Shen, W. Liu, Y. Chen, *Anal. Chem.*, 2007, **79**, 5862-5868.

13 M. Kim, J. Stripeikis, M. Tudino, *Spectrochimica Acta Part B*, 2009, **64**, 500-505.

14 P. A. Sule, J. D. Ingle, Jr., *Analytica Chimica Acta*, 1996, **326**, 85-93.

15 A. H. El-Sheikh, Y. S. Al-Degs, J. A. Sweileh, A. J. Said, *Talanta*, 2013, **116**, 482-487.

16 R. A. Gil, S. Cerutti, J. A. Gasquez, R. A. Olsina, L. D. Martinez, *Talanta*, 2006, **68**, 1065-1070.

17 R. C. Bolzan, L. F. Rodrigues, J. C. Paz de Mattos, V. L. Dressler, E. Marlon de Moraes Flores, *Talanta*, 2007, **74**, 119-124.

18 A. Baysal, S. Akman, S. Demir, M. Kahraman, *Microchemical Journal*, 2011, **99**, 421-424.

19 S. Sadeghi, A. Z. Moghaddam, *Talanta*, 2012, **99**, 758-766.

20 T. Sumida, T. Ikenoue, K. Hamada, A. Sabarudin, M. Oshima, S. Motomizu, *Talanta*, 2005, **68**, 388-393.

21 T. Sumida, A. Sabarudin, M. Oshima, S. Motomizu, *Analytical Sciences*, 2006, **22**, 161-164.

22 M. Stanislawska, B. Janasik,W. Wasowicz, *Talanta*, 2013, **117**, 14-19.

23 M, F. Bergamini, D. P. dos Santos, M. V. B. Zanoni, *Sensors and Actuators B*, 2007, **123**, 902–908.

24 R. T. Kachoosangi, R. G. Compton, *Sensors and Actuators B*, 2013, **178**, 555–562.

25 S. J. Toal, K. A. Jones, D. Magde, W. C. Trogler, *J. Am. Chem. Soc.*, 2005, **127**, 11661-11665.

26 B. Gammelgaard, Yi-ping Liao, O. Jons, *Analytica Chimica Acta*, 1997, **354**, 107-113.

27 Hong-Bing Fu, Jian-Nian Yao, *J. Am. Chem. Soc.*, 2001, **123**, 1434-1439.

28 Y. Lei, Q. Liao, H. Fu, J. Yao, *J. Phys. Chem. C*, 2009, **113**, 10038–10043.

29 J. Wang, Y. Zhao, J. Zhang, J. Zhang, B. Yang, Y. Wang, D. Zhang, H. You, D. Ma, *J. Phys. Chem. C*, 2007, **111**, 9177-9183.

30 A. G. L. Olive, A. D. Guerzo, C. Schafer, C. Belin, G. Raffy, C. Giansante, *J. Phys. Chem. C*, 2010, **114**, 10410-10416.

31 E. Kwon, H. Oikawa, H. Kasai, H. Nakanishi, *Crystal Growth & Design,* 2007, **7**, 600-602.

32 Byeong-Kwan An, Soon-Ki Kwon, Sang-Don Jung, Soo Y. Park, *J. Am. Chem. Soc.,* 2002, **124**, 14410-14415.

33 S. Li, L. He, F. Xiong, Y. Li, G. Yang, *J. Phys. Chem. B*, 2004, **108**, 10887-10892.

34 Y. Jie, W. Rui, D. Ran, L. Ai-wu, Y. Yong-sen, W. Ji-ping, Y. Han, *Chem. Res. Chinese Universities*, 2011, **27**, 1045-1048.

35 L. Kang, Z. Wang, Z. Cao, Y. Ma, H. Fu, J. Yao, *J. Am. Chem. Soc.*, 2007, **129**, 7305-7312.

36 J. Lyklema, *Fundamentals of Interface and Colloid Science*, Elsevier, Wageningen, 1995.

37 A. H. Gore, U. Sh. Mote, S. S. Tele, P. V. Anbhule, M. C. Rath, S. R. Patil, G. B. Kolekar, *Analyst*, 2011, **136**, 2606.

38 C. M. Spillmann, J. Naciri, G. P. Anderson, Mu-San Chen, B. R. Ratna, *nano*, 2009, **3**, 3214-3220.

39 L. Wang, L. Wang, T. Xia, L. Dong, G. Bian, H. Chen, *Analytical Sciences*, 2004, **20**, 1013-1017.

40 S. She, Y. Zhou, L. Zhang, L. Wang, L. Wang, *Spectrochimica Acta Part A*, 2005, **62**, 711–715.

41 L. Wang, T. Xia, J. Liu, L. Wang, H. Chen, L. Dong, G. Bian, *Spectrochimica Acta Part A*, 2005, **62**, 565–569.

42 L. Wang, L. Wang, T. Xia, L. Dong, H. Chen, L. Li, *Spectrochimica Acta Part A*, 2004, **60**, 2465–2468.

Figure captions:

Fig. 1 (a) Particle size distribution histograms of PNPs in aqueous suspension in the absence of surfactant and (b) presence of CTAB surfactant.

Fig. 2 Representation of zeta potential of the PNPs without and with surfactants.

Fig. 3a SEM photomicrograph of PNPs in absence of CTAB surfactant.

Fig. 3b SEM photomicrograph of PNPs in presence of CTAB surfactant.

Fig. 4 UV-Vis absorption spectra of PNPs in aqueous dispersion (spectrum A) and homogeneous solution of perylene in acetone (spectrum B).

Fig. 5 FL emission spectrum of dilute solution of perylene in acetone (dotted line) monitored at excitation wavelength, λ_{ex} = 410 nm and that of PNPs in aqueous suspension (solid line) at excitation wavelength, λ_{ex} = 382 nm.

Fig. 6a Excitation (A) and FL (B) spectra of PNPs suspension.

Fig. 6b Excitation (C) and FL (D) spectra for perylene in acetone.

Fig. 7 Effect of pH on FL intensity (λ_{em} = 572 nm) of PNPs suspension (λ_{ex} = 382 nm).

Fig. 8 FL intensity response [ΔF/F] in the presence and absence of the Cr(VI) specie and various co-existing ions like Cr(III), Al(III), Ba(II), Fe(III), Zn(II), Na(I), Hg(II), Ni(II), Cu(II), Co(II), K(I), NO_3^-, Cl^-, SO_4^{2-}, CO_3^{2-}, BrO_3^-, IO_3^-, ClO_3^- (50 μg mL^{-1})

Fig. 9 FL spectra of PNPs suspension (1 μg mL^{-1}) in the presence of increasing concentration of dichromate ions (0, 1, 2, 3, 4, 5, 6, 7, 8, 9, 16, 32, 50 μg mL^{-1})

Fig.10 Stern-Volmer plot of fluorescence quenching data of PNPs with addition of different amounts of Cr(VI) ion solution.

Scheme 1 Proposed graphic for formation of CTAB-PNPs and its surface bound non- fluorescent stable micellar complex with dichromate ions.

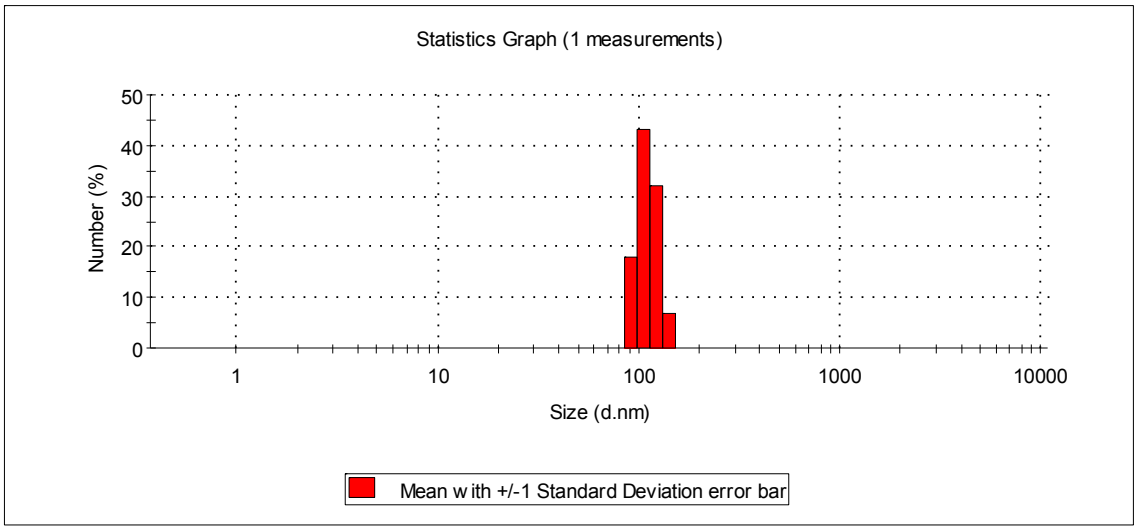

Fig. 1a

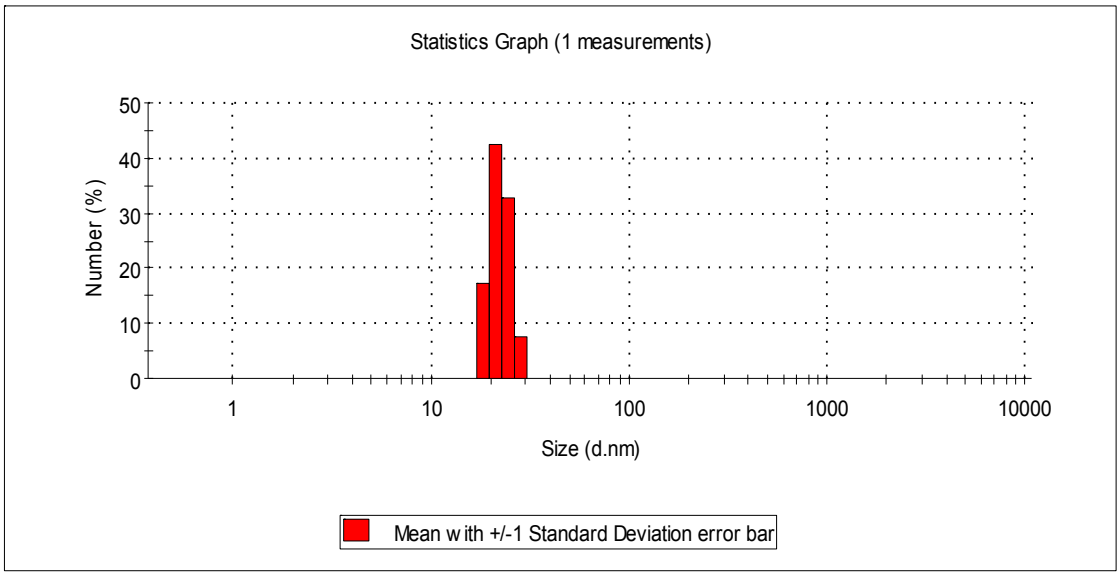

Fig. 1b

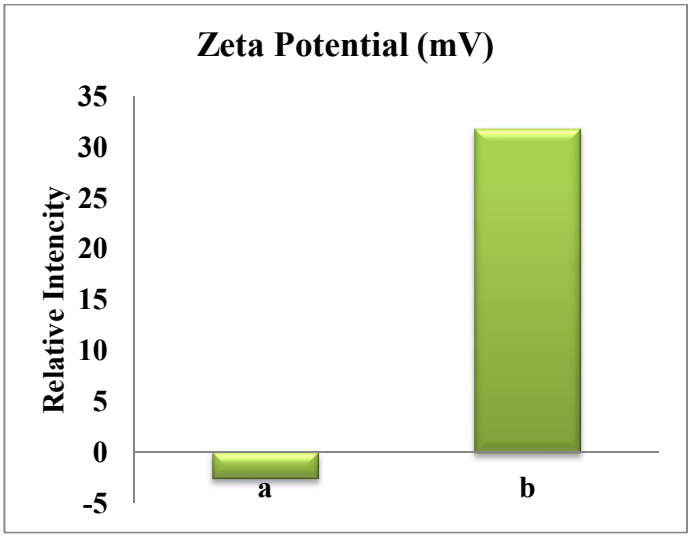

Fig. 2

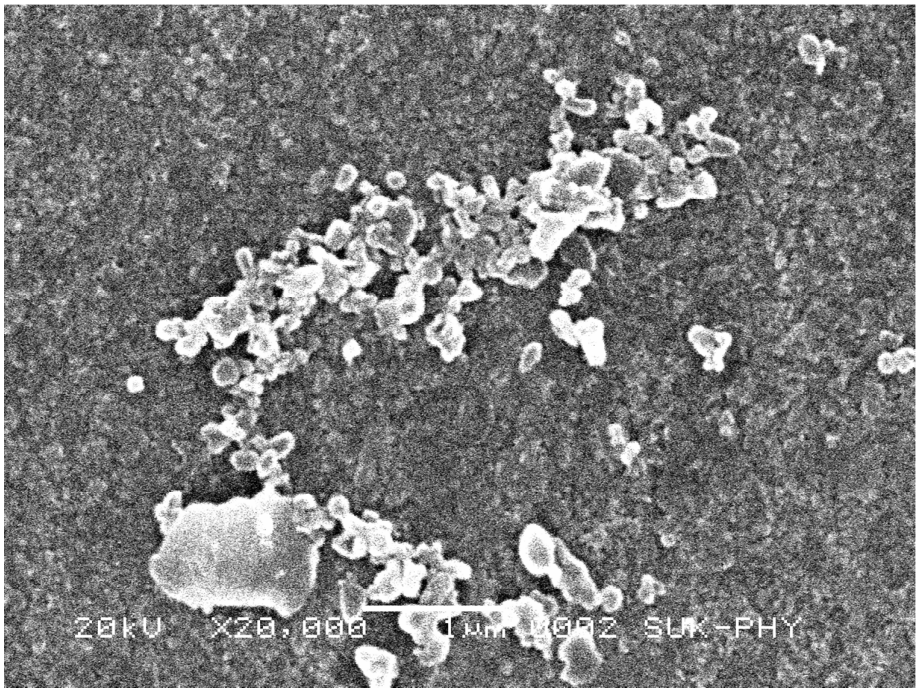

Fig. 3a

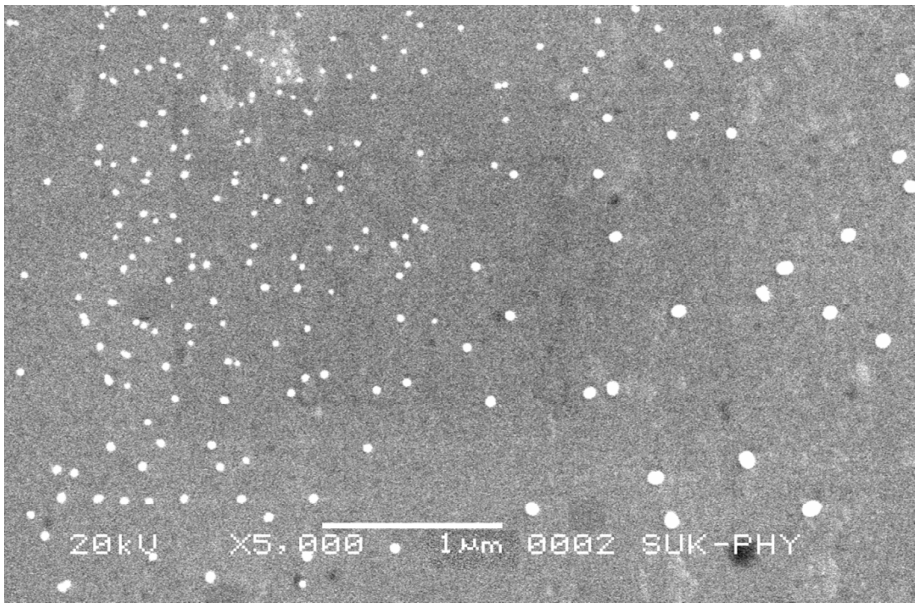

Fig. 3b

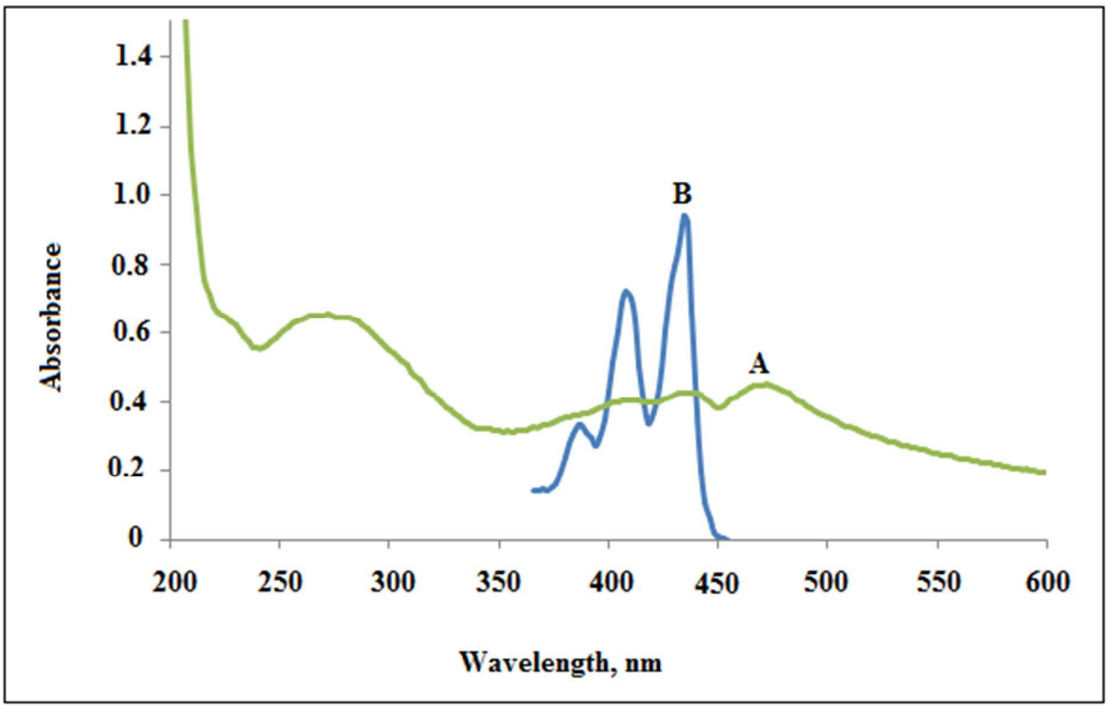

Fig. 4

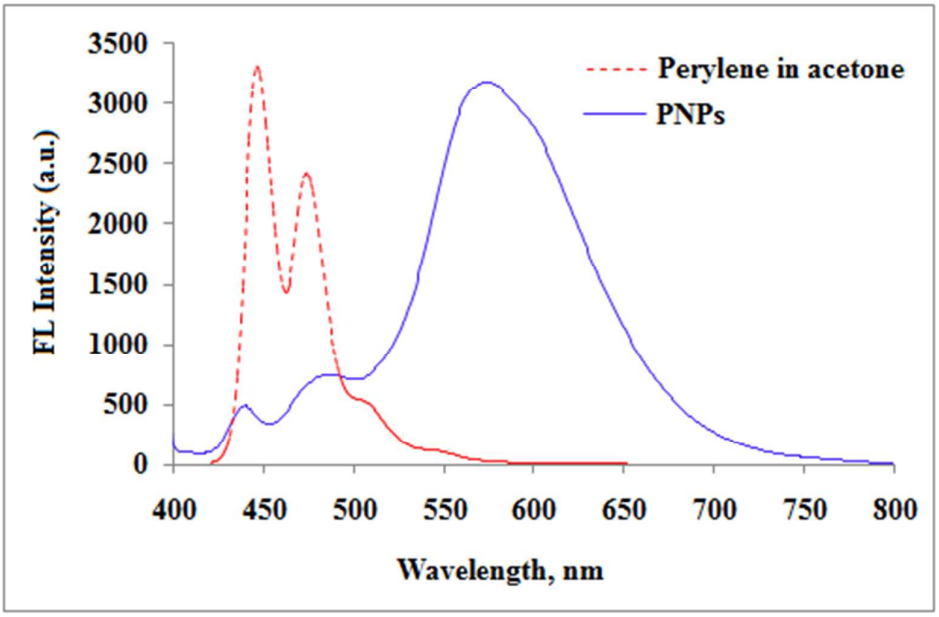

Fig. 5

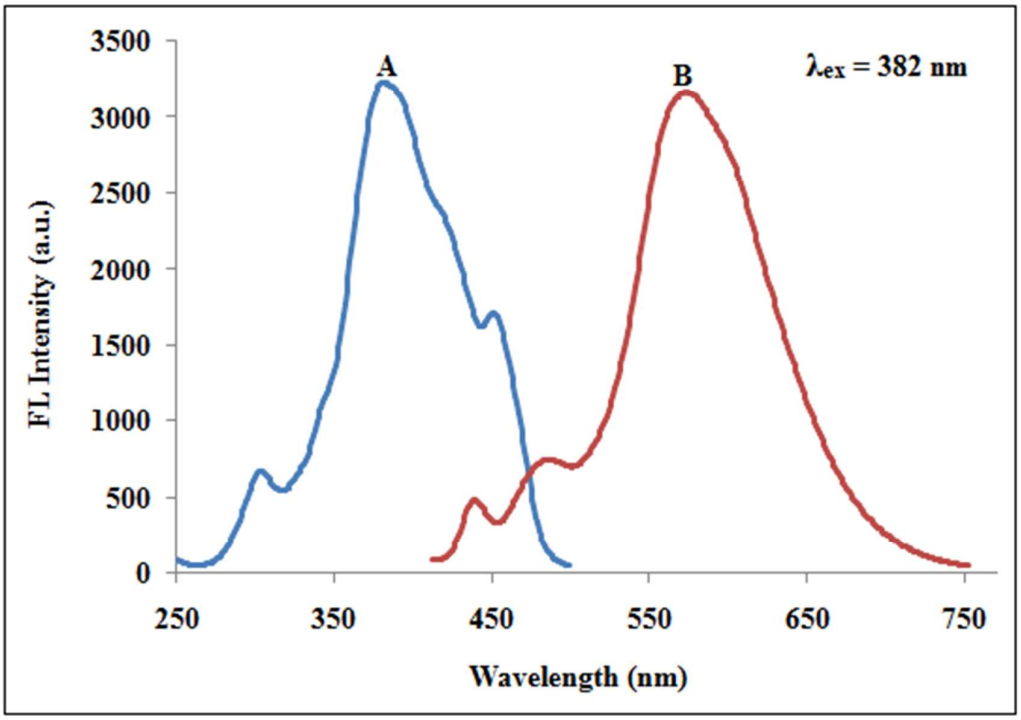

Fig. 6a

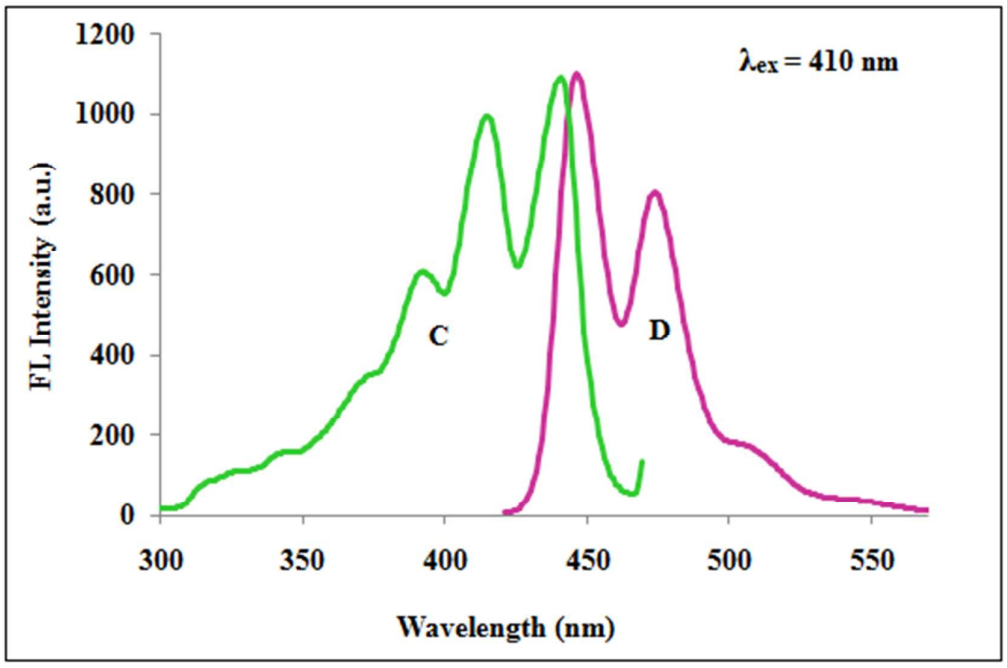

Fig.6b

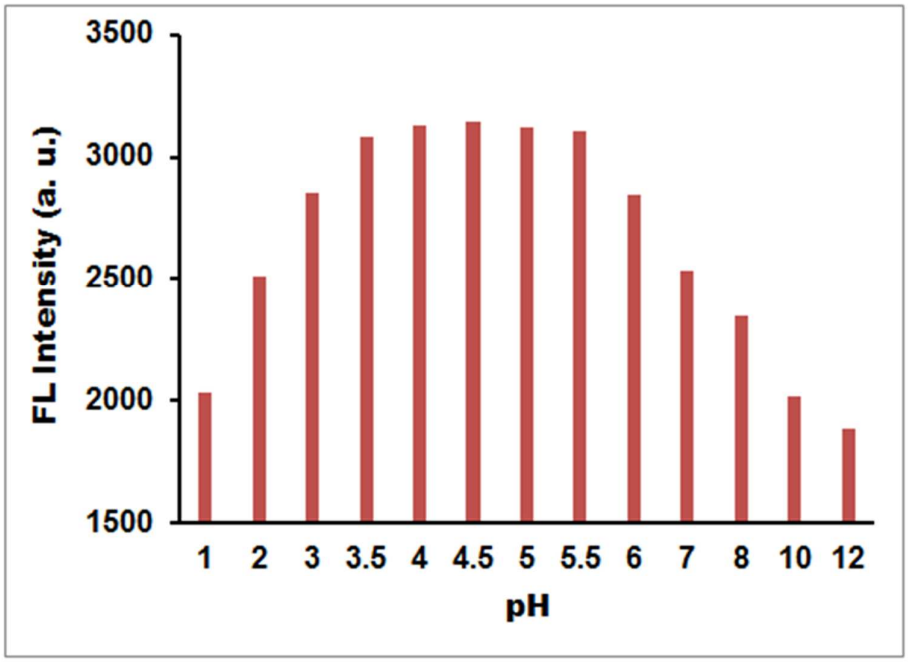

Fig. 7

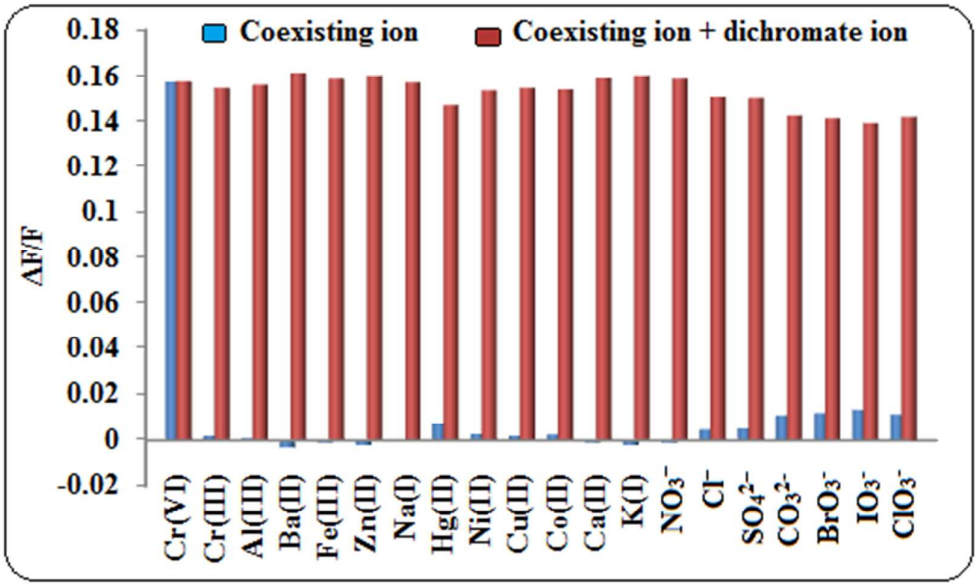

Fig. 8

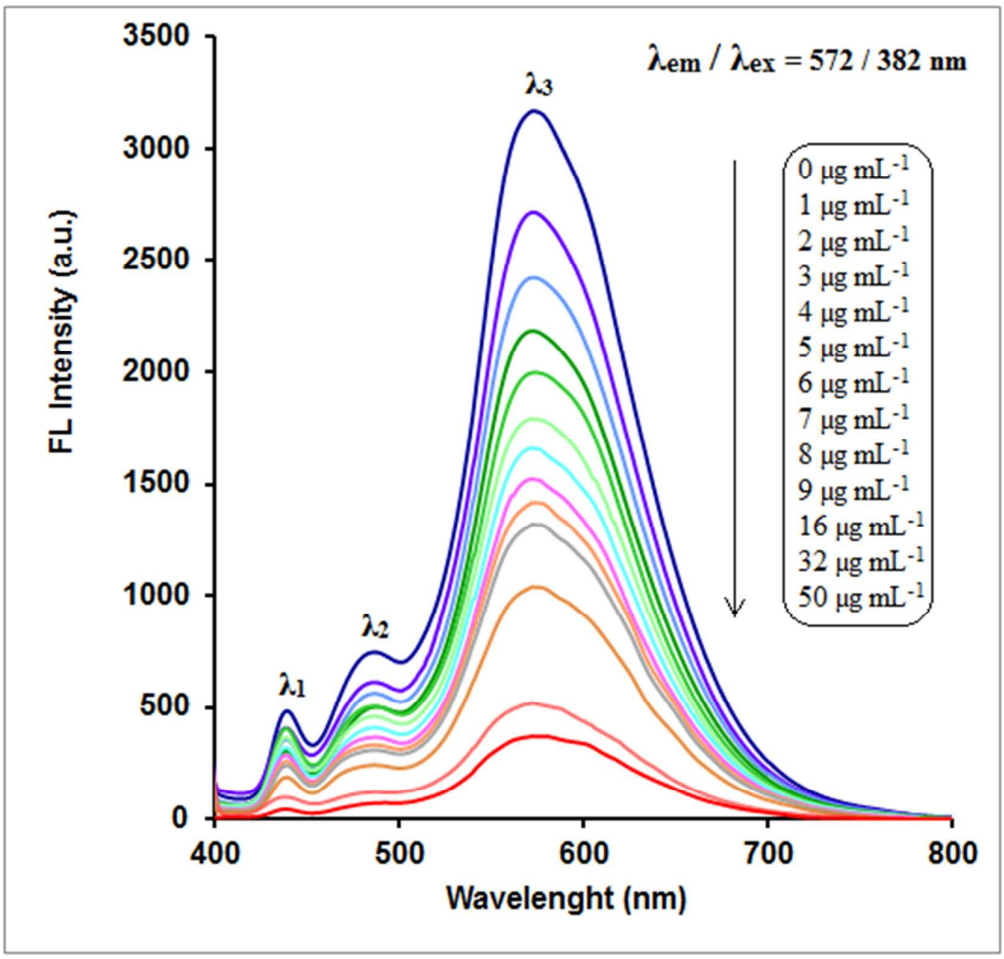

Fig. 9

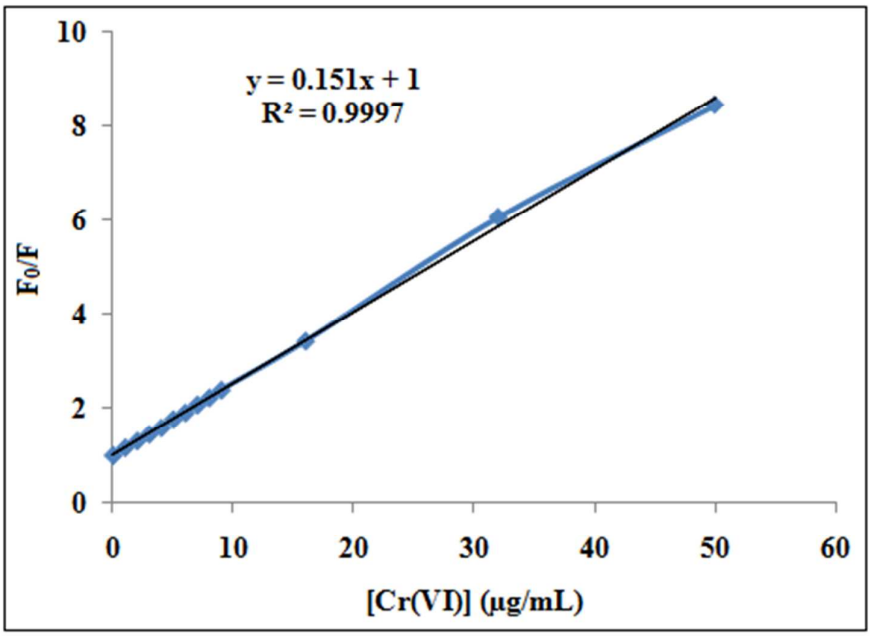

Fig. 10

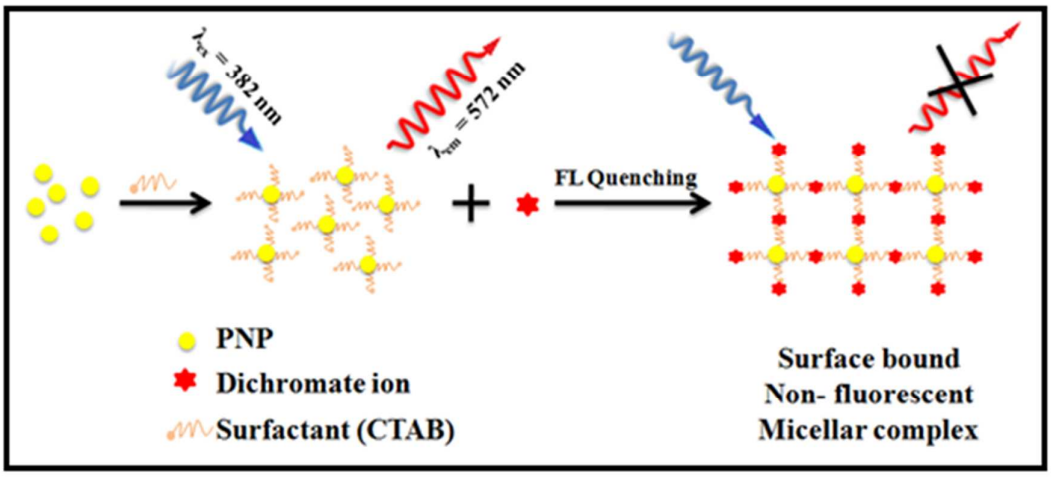

Scheme 1 Proposed graphic for formation of CTAB-PNPs and its surface bound non-fluorescent stable micellar complex with dichromate ions.

Table Captions

Table 1. Comparison the analytical performances the methods based on FL quenching of different NPs for detection of Cr(VI).

Reagents	LOD	Linear Range	Reference No.
1-Pyrenemethylamine organic nanoparticles	2.8 μmol L^{-1}	7-100 μmol L^{-1}	[39]
Polyvinyl alcohol keto-derivatives Nanoparticles	0.02 μg mL^{-1}	0.1–13.2 μg mL^{-1}	[40]
Anthracene/poly-acrylamide (AN/PAM) nanoparticles	0.02 μg mL^{-1}	0.04-2.0 μg mL^{-1}	[41]
Poly-4-vinylaninline nanoparticles	0.02 μg mL^{-1}	0.1–13.0 μg mL^{-1}	[42]
Perylene nanoparticles	**0.008 μg mL^{-1}**	**0.5- 50 μg mL^{-1}**	**Proposed method**

Table 2. Determination of Cr(VI) in synthetic samples

Cr(III) in samples (μg mL^{-1})	Cr(VI) in samples (μg mL^{-1})	Cr(VI) found* (μg mL^{-1})	Recovery, %	RSD, %
2	2	2.003	100.15	0.019
4	2	1.998	99.90	0.018
6	2	2.000	100	0.020

*Average of four determinations.

Table 3. Determination of Cr(VI) in different environmental water samples

Water samples ($\mu g\ mL^{-1}$)	Cr(VI) found in water samples* ($\mu g\ mL^{-1}$)		Recovery, %	RSD, %
	AAS Method	The Present Method		
Industrial waste-water No. 1	1.02	1.006	100.3	0.020
Industrial waste-water No. 2	2.05	1.998	99.22	0.021
Drinking Water	Not detected	Not detected	-	-
Mineral Water	Not detected	Not detected	-	-

*Average of four determinations.